

UNCLASSIFIED

AD NUMBER

AD850882

NEW LIMITATION CHANGE

TO

**Approved for public release, distribution
unlimited**

FROM

**Distribution authorized to U.S. Gov't.
agencies and their contractors;
Administrative/Operational Use; Mar 1969.
Other requests shall be referred to Air
Force Weapons Lab., Kirtland AFB, NM
87117.**

AUTHORITY

AFWL ltr, 30 Nov 1971

THIS PAGE IS UNCLASSIFIED

AD850882

AFWL-TR-69-11

AFWL-TR-
69-11

THE INCLUSION OF STRAIN-RATE DEPENDENCE IN THE PUFF COMPUTER CODE

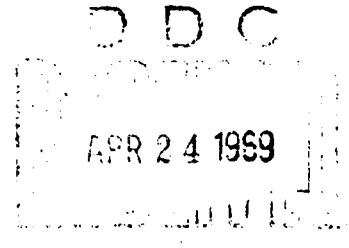


Joseph B. Webster III

Capt USAF

TECHNICAL REPORT NO. AFWL-TR-69-11

March 1969



AIR FORCE WEAPONS LABORATORY
Air Force Systems Command
Kirtland Air Force Base
New Mexico

This document is subject to special export controls and each transmittal to foreign governments or foreign nationals may be made only with prior approval of AFWL (WLRP) , Kirtland AFB, NM, 87117.

AFWL-TR-69-11

THE INCLUSION OF STRAIN-RATE DEPENDENCE
IN THE PUFF COMPUTER CODE

Joseph B. Webster III
Captain USAF

TECHNICAL REPORT NO. AFWL-TR-69-11

This document is subject to special export controls and each transmittal to foreign governments or foreign nationals may be made only with prior approval of AFWL (WLRP), Kirtland AFB, NM 87117. Distribution is limited because of the technology discussed in the report.

ACCESSION FOR	WHITE SECTION <input type="checkbox"/>
CFSTI	BUFF SECTION <input checked="" type="checkbox"/>
BCC	<input type="checkbox"/>
UNANNOUNCED	<input type="checkbox"/>
JUSTIFICATION
BY	
DISTRIBUTION/AVAILABILITY CODES	
DIST.	AVAIL. and/or SPECIAL
2	

AIR FORCE WEAPONS LABORATORY
Air Force Systems Command
Kirtland Air Force Base
New Mexico

When U. S. Government drawings, specifications, or other data are used for any purpose other than a definitely related Government procurement operation, the Government thereby incurs no responsibility nor any obligation whatsoever, and the fact that the Government may have formulated, furnished, or in any way supplied the said drawings, specifications, or other data, is not to be regarded by implication or otherwise, as in any manner licensing the holder or any other person or corporation, or conveying any rights or permission to manufacture, use, or sell any patented invention that may in any way be related thereto.

This report is made available for study with the understanding that proprietary interests in and relating thereto will not be impaired. In case of apparent conflict or any other questions between the Government's rights and those of others, notify the Judge Advocate, Air Force Systems Command, Andrews Air Force Base, Washington, D. C. 20331.

DO NOT RETURN THIS COPY. RETAIN OR DESTROY.

FOREWORD

This research was performed under Program Element 61102A, Project 5710, Subtask AA106, and was funded by the Defense Atomic Support Agency (DASA).

Inclusive dates of research were September 1968 through January 1969. The report was submitted 31 January 1969 by the Air Force Weapons Laboratory Project Officer, Captain Joseph B. Webster III (WLRP).

Information in this report is embargoed under the U.S. Export Control Act of 1949, administered by the Department of Commerce. This report may be released by departments or agencies of the U.S. Government to departments or agencies of foreign governments with which the United States has defense treaty commitments, subject to approval of AFWL (WLRP).

This technical report has been reviewed and is approved.

Capt Joseph B. Webster III
JOSEPH B. WEBSTER III
Captain, USAF
Project Officer

Donald A. Shulkin
HARRY F. RIZZO
Lt Colonel, USAF
Chief, Physics Branch

Claude K. Stambaugh
CLAUDE K. STAMBAUGH
Colonel, USAF
Chief, Research Division

ABSTRACT

(Distribution Limitation Statement No. 2)

Two mathematical descriptions of the strain-rate dependence of materials response to suddenly applied one-dimensional strain loads were incorporated into the PUFF wave propagation computer codes. The models are quite different in that one uses a macroscopic relaxation time to govern the stress-relaxation rates, while the other uses the microscopic theories of dislocation dynamics. The results of several sample calculations are discussed, and the changes required in the programming sequence are given. Some comments are provided concerning the validity and usefulness of these models, and a brief analysis of the effects of parametric variations is presented.

CONTENTS

<u>Section</u>		<u>Page</u>
I	INTRODUCTION	1
II	DISLOCATION DYNAMICS MODEL	3
	Mathematical Dependence of Parameters	5
	Inclusion of Incremental Shear Strain	7
	Comparison with Local Shear Strain Calculation	10
III	STRESS-RELAXATION MODEL	13
	Test Problems	15
	Programming Changes in PUFF	15
IV	DISCUSSION	18
V	CONCLUSIONS	20
	Appendix	21
	References	32
	Distribution	33

ILLUSTRATIONS

<u>Figure</u>		<u>Page</u>
1	Flow Schematic of Stress Strain Calculation	2
2	Average Dislocation Velocity versus Resolved Shear Stress	6
3	Dependence of N on γ and δ	8
4	Comparison Between Waveforms Generated by Various Dislocation Models	12
5	Effect of Relaxation Time Upon a Transmitted Waveform	16
6	Stress-Strain Routine Modified to Include Macroscopic Relaxation and Dislocation Dynamics Models for Strain-Rate Dependence	17
7	Illustration of the Effect of the Initial Value of Plastic Shear Strain on a Propagated Waveform	19
8	Stress-Distance Histories for Incremental Shear Strain Problem	22
9	Stress-Distance Histories for Incremental Shear Strain Problem	23
10	Stress-Distance Histories for Incremental Shear Strain Problem	24
11	Stress-Distance Histories for Incremental Shear Strain Problem	25
12	Stress-Distance Histories for Incremental Shear Strain Problem	26
13	Stress-Distance Histories for Local Shear Strain Problem	27
14	Stress-Distance Histories for Local Shear Strain Problem	28
15	Stress-Distance Histories for Local Shear Strain Problem	29
16	Stress-Distance Histories for Local Shear Strain Problem	30
17	Stress-Distance Histories for Local Shear Strain Problem	31

SECTION I

INTRODUCTION

The PUFF 66 and P PUFF 66 computer codes were developed to describe the shocks resulting from thermally and mechanically induced loads on semi-infinite slabs of material (Reference 1). These codes, which compute one-dimensional motion, are based upon the principles of fluid dynamics, or "hydrodynamic" motion. The first logical improvement in their degree of sophistication was the inclusion of material strength in shear. This was performed after the elastic-plastic formulation by Wilkins (Reference 2), and includes the von Mises stress-dependent yield criterion. The next logical step in upgrading these codes toward more realistic descriptions of material behavior is the inclusion of a rate dependent description of dynamic yielding.

Two models for strain-rate dependent yielding have been programmed into the PUFF 66 running system, and either or both may be employed in a given problem; however, only one description should be used per material. The first model is based upon the formulation proposed by Taylor (Reference 3) to explain dynamic yielding through a phenomenological description of dislocation motion in metals. The other is a macroscopic description proposed by Alverson and Hannagud (Reference 4). The adaptation of each model is presented in the following sections with comments about their use in running a problem.

The models were incorporated to give the user of the PUFF 66 codes an option that would allow the use of the von Mises yield criterion or, depending upon one's knowledge of the material, the use of a model whose degree of sophistication ranges from a single parameter in the macroscopic relaxation model to a microscopic model based upon dislocation dynamics. The changes in programming occur in the stress-strain calculation of the HYDRO subroutine; this is shown by the flow schematic of figure 1.

The following sections briefly describe the theories outlined in References 3 and 4, along with comments about the effects imposed upon the wave propagation calculations by these descriptions. These effects are additionally displayed by the results of selected calculations performed with each model. The user of these material descriptions is urged to read References 3 and 4 before implementing these changes to the PUFF codes.

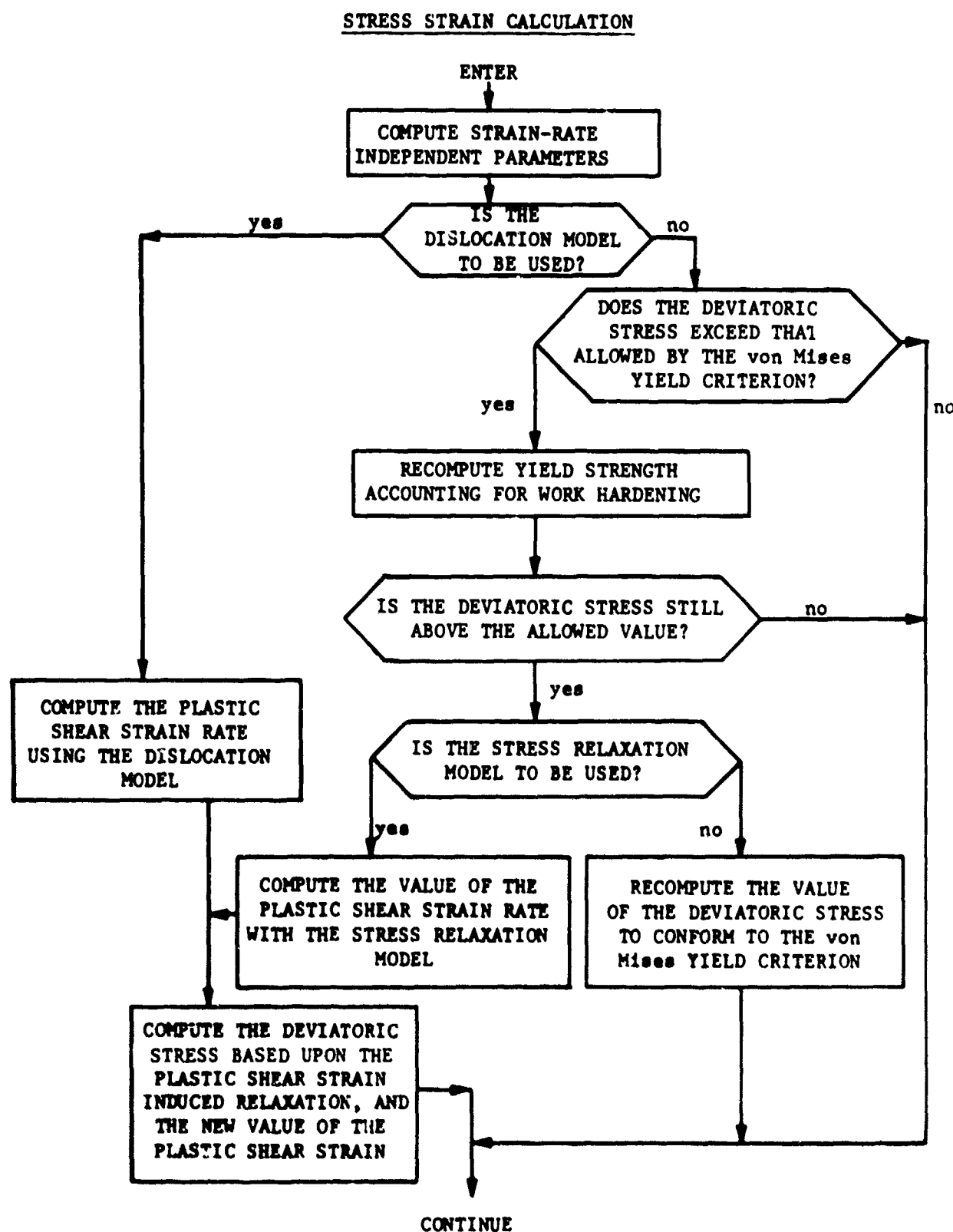


Figure 1. Flow Schematic of Stress Strain Calculation

SECTION II
DISLOCATION DYNAMICS MODEL

The dislocation model of Gilman and Johnston (Reference 5) as adapted by Taylor to describe dynamic yielding phenomena is a more sophisticated treatment than those yield descriptions based only upon stress considerations. This yielding occurs when the shear stresses on linear defects in a material's structure are sufficient to cause the structure to deform to some arrangement that requires a lesser stress to maintain the imposed total strain. In plastic deformation of crystalline materials, the theory of dislocation motion was postulated, and has since been verified, as the mechanism for plastic deformation of materials under shear stresses. The model combines elastic response with a strain-rate controlled relaxation to hydrodynamic or plastic behavior. Upon initial loading, and before plastic deformation has occurred, the material has not reformed its structure to relieve stress loads, and the shear stresses are at their maximum value for the imposed total strain. The average dislocation velocity is a function of the resolved shear stress, and the rising shear stress produces plastic shear strain through dislocation motion. The deformation work in the material will produce new dislocations, and the resulting higher dislocation density coupled with a large average dislocation velocity produces the rate of relaxation of the total stress. When the relaxation rate and the strain rate become matched, the material can attain an equilibrium stress-strain state. This state will, in general, lie above the material's hydrostat, and is the Hugoniot state one would measure in an impact experiment.

For this model Taylor derives the relation for the normal stress in one-dimensional strain as

$$\sigma_n = (\lambda + 2\mu) \epsilon_n^T - \frac{8}{3} \mu \gamma \quad (1)$$

where σ_n is the normal stress, λ and μ are the Lamé constraints, ϵ_n^T is the total normal strain, and γ is the plastic shear strain. By using the expression for the time dependence of the plastic shear strain, one obtains

$$\frac{d\gamma}{dt} = bNv \quad (2)$$

where b is the Burgers vector, N the mobile dislocation density or the total dislocation length per cubic centimeter and v the average dislocation velocity. The relations which Taylor uses for N and v are

$$N = N_0 + \alpha \gamma^\beta \quad (3)$$

and

$$v = v_\infty e^{-\frac{\tau_0 + \phi \gamma}{\tau}} \quad (4)$$

where N_0 is the initial dislocation density, α and β are constants measured for several materials by Keh and Weissman (Reference 6), v_∞ is normally taken as the acoustic shear velocity, τ_0 is a constant, ϕ is a work hardening term, and τ is the resolved shear stress. One may derive expressions for the plastic shear strain and resolved shear stress at 45° to the propagation direction as

$$\gamma = \frac{3}{8\mu} \left[(\lambda + 2\mu)\epsilon - \sigma \right] \quad (5)$$

and

$$\tau = \frac{3}{4} \left[\sigma - \left(\lambda + \frac{2}{3} \mu \right) \epsilon \right] \quad (6)$$

Taylor's equation for the time dependence of the total stress, based upon stress being positive in tension, is

$$\sigma = -P + S_d$$

as in the Wilkins formulation for the elastic-plastic flow (Reference 2). This expression can be rewritten to allow strain-rate dependence of the deviator only, using the PUFF 66 convention of stress, which is positive in compression. Since the hydrostatic component of the stress may be written as

$$P = \left(\lambda + \frac{2}{3} \mu \right) \epsilon$$

the stress deviator from Eq. (1) is now in strain-rate dependent form:

$$\dot{S}_d = \frac{4}{3} \mu \dot{\epsilon} - \frac{8}{3} \mu \dot{\gamma} \quad (7)$$

In the PUFF formulation $\dot{\epsilon}$ becomes $-\frac{\dot{v}}{v}$ and

$$\dot{s}_d = -\frac{4}{3} \mu \frac{\dot{v}}{v} - \frac{8}{3} \mu \dot{\gamma}$$

By combining Eq. (3) and (4) with the expression for $\dot{\gamma}$ in Eq. (2), one has

$$\dot{s}_d = -\frac{4}{3} \mu \frac{\dot{v}}{v} - \frac{8}{3} \mu b \left[N_o + \alpha \gamma^3 \right] v_\infty e^{-\frac{\tau_o + \phi \gamma}{\tau}}$$

By using the PUFF convention for calculating stress where

$$\dot{\sigma} = \dot{P} - \dot{s}_d$$

this equation becomes

$$\dot{s}_d = \frac{4}{3} \mu \frac{\dot{v}}{v} + \frac{8}{3} \mu b v_\infty \left[N_o + \alpha \gamma^3 \right] e^{-\frac{\tau_o + \phi \gamma}{\tau}}$$

By incorporating the expression for γ and τ in Eq. (5) and (6) one may write the equation for the time-rate-of-change of the deviatoric stress as

$$\dot{s}_d = \frac{4}{3} \mu \frac{\dot{v}}{v} + \frac{8}{3} \mu b v_\infty \left\{ N_o + \alpha \left[\frac{3}{8\mu} [(\lambda + 2\mu)\epsilon - \sigma] \right]^3 \right\} \times \xi$$

$$\xi = \left(\exp - \left\{ \tau_o + \frac{3}{8\mu} [(\lambda + 2\mu)\epsilon - \sigma] \right\} / \frac{3}{4} [\sigma - (\lambda + 2/3 \mu)\epsilon] \right) \quad (8)$$

1. Mathematical Dependence of Parameters

The physical parameters included in the final equation for this model are numerous, and one might expect them all to affect the calculations in a manner that would be difficult to allow a parametric sensitivity study to shed light on the specific effect each parameter would have upon the calculations. It is a good idea, therefore, to look at the actual expressions in some detail to get a better understanding of the effects of the parameters.

Starting with Eq. (1), one sees that this can be broken down to a thermodynamic P-V-E state and a shear strain-rate dependent deviatoric stress component:

$$\dot{\sigma} = \dot{P} - \frac{4}{3} \mu \frac{\dot{v}}{v} - \frac{8}{3} \mu \dot{\gamma} \quad (9)$$

The $8/3 \dot{\gamma}^2$ term simply relates the extent of reformation of material structure to the rate of relaxation of the total normal stress in a one-dimensional strain calculation. Returning to the initial expression for shear strain rate,

$$\dot{\gamma} = bNv$$

the product of the three terms is simply the volume of slippage, or deformation, which has occurred in the material per unit volume, per unit time. One must now evaluate the shear stress and shear strain dependence of N and v to determine the shear strain-rate.

The formulation used to evaluate the average dislocation velocity v , is given by Eq. (4). This is a continuously varying function of the type shown in figure 2. One notes that the average dislocation velocity asymptotically approaches the value v_∞ , and therefore could never reach this maximum in a normal calculation. The work-hardening term in Eq. (4) is included to account for the interactions of the dislocations with each other. There are a number of postulated

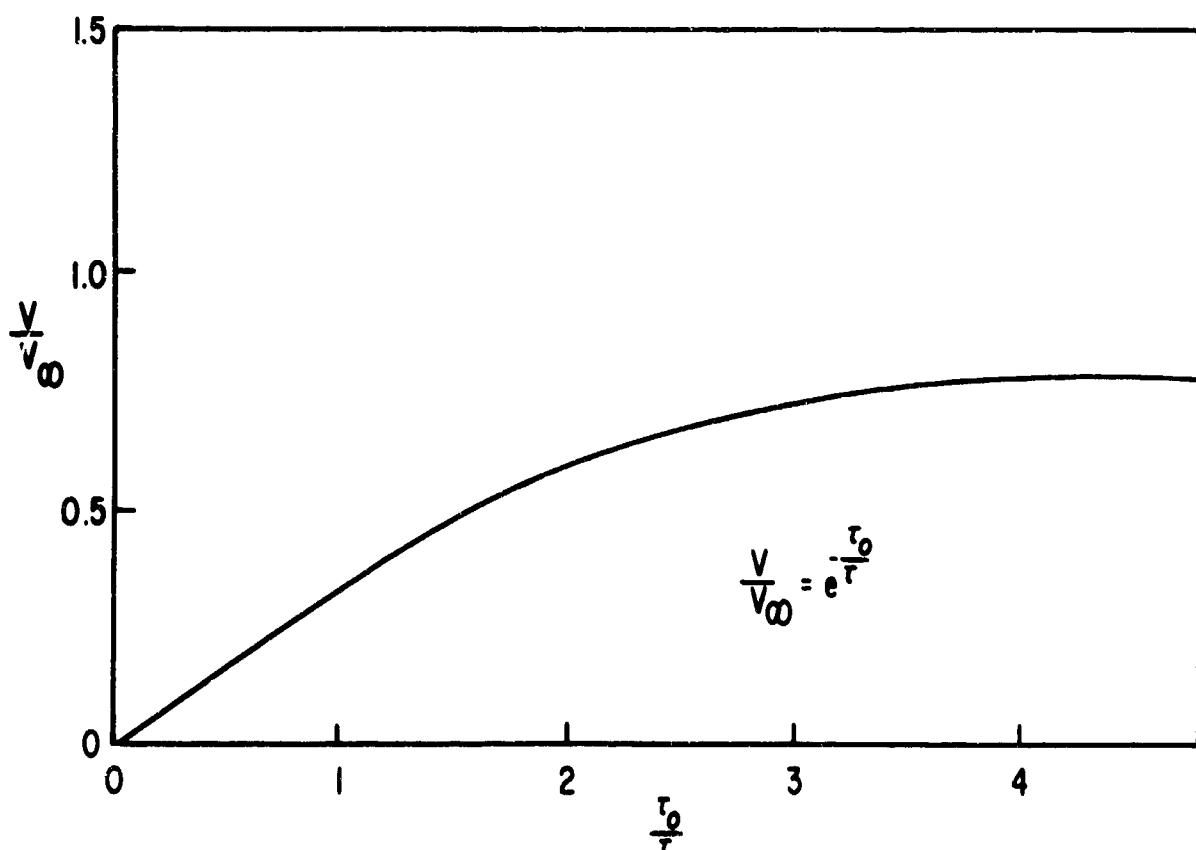


Figure 2. Average Dislocation Velocity versus Resolved Shear Stress

physical mechanisms that may occur; however, their overall effect should be thought of as increasing the resolved shear stress required to produce a given average dislocation velocity.

The change in the number of dislocations present in the material is generally a function of the deformation work being done on the material, and is expressed for this model in Eq. (3) as

$$N = N_0 + \alpha \gamma^\beta$$

The coefficient β has been generally determined to fall between the values of 0.5 and 1.5 by Keh and Weissman (Reference 6). As the plastic shear strain, γ , will have a value much less than 1, one can see that the rate of increase in dislocation density is inversely proportional to β . Thus the rate of relaxation is inversely proportional to β , and directly proportional to α if all other quantities in Eq. (8) are fixed. Since this is not the case in a dynamic calculation, these parameters, along with the others, should only be evaluated in a qualitative sense. The dependence of N on β and γ is illustrated in figure 3.

One should notice in this formulation several things that indicate that it is restricted to use in compression, pending some modifications. First, the plastic shear strain should be written as a differential quantity if subsequent unloading is to be handled. Second, one sees that the stress is always driven toward tension as currently formulated, and can cause the unloading to be unbounded without constraints. This could be corrected by checking to determine if the material is unloading, and then forcing the time dependent term to drive the stress deviator toward the hydrostat. Another method would be to use the normal von Mises yield criterion in unloading.

2. Inclusion of Incremental Shear Strain

By allowing the calculation to handle plastic shear strain as an incrementally increasing function, one eliminates the need for using the dislocation model only during compressive loading. The changes necessary to perform this type of calculation are relatively straightforward and involve only a few additional statements in the calculation sequence. The terms affected are the plastic shear strain and the resolved shear stress calculations.

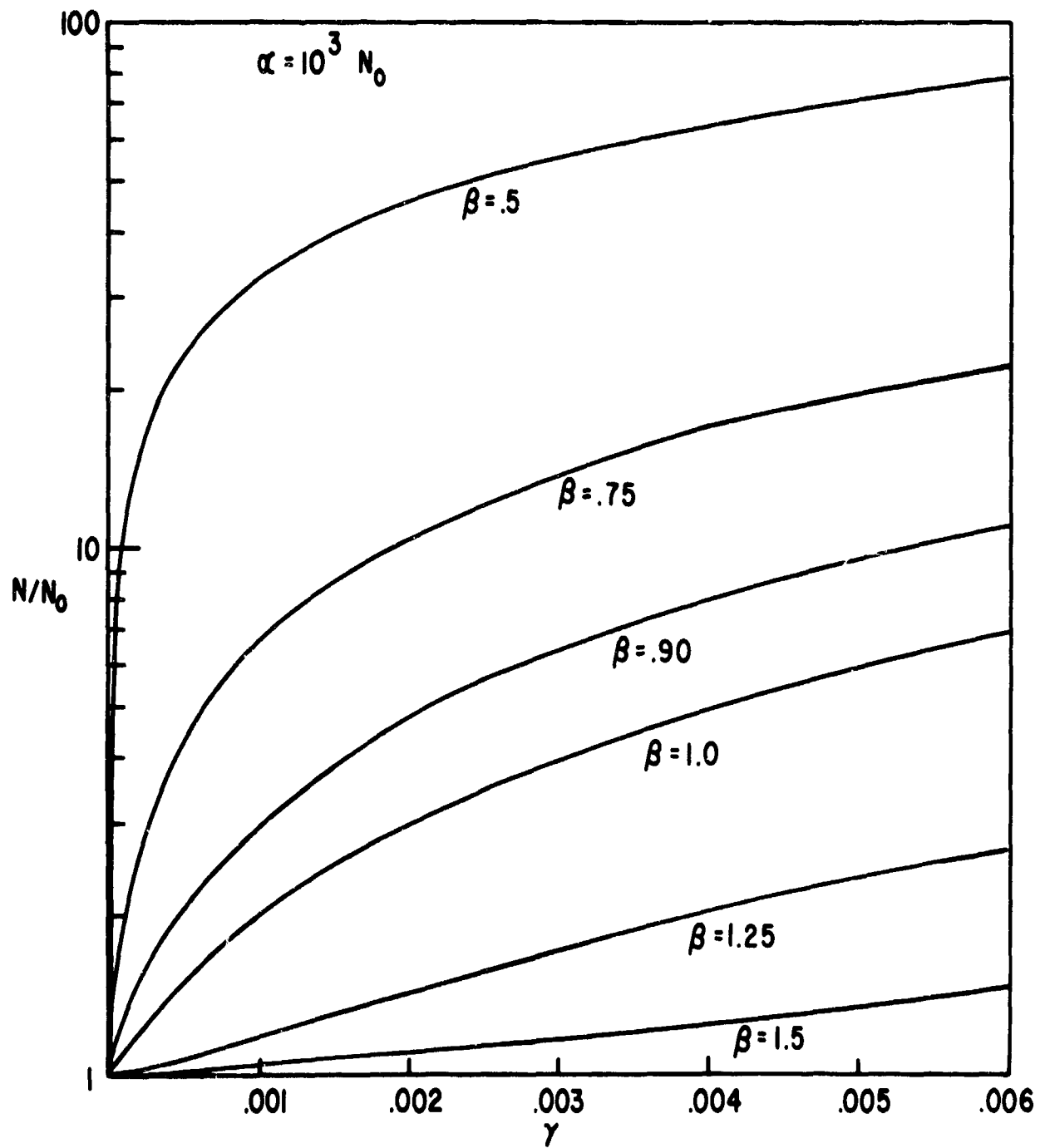


Figure 3. Dependence of N on γ and β

The resolved shear stress as currently calculated in Eq. (6) must be modified to become positive in both compressive loading and unloading, as the expression for average dislocation velocity otherwise becomes unbounded. Physically this modification simply says that the amount of plastic shear strain is a scalar quantity, and that a revolved shear stress, tensile or compressive, results in dislocation motion. Equation (6) is rewritten as

$$\tau = \frac{3}{4} \text{ ABS} \left[\sigma - \left(\lambda + \frac{2}{3} \mu \right) \epsilon \right] \text{ or, } \frac{3}{4} \text{ ABS} \left[s_d \right] \quad (10)$$

The plastic shear strain is now a quantity that must increase on loading and unloading, and is calculated by

$$\gamma^{n+1} = \gamma^n + \Delta\gamma \quad (11)$$

The increase, $\Delta\gamma$, must therefore be calculated at each time increment, n , and can be written

$$\Delta\gamma^{nH} = \gamma^{n+1} - \gamma^n \quad (12)$$

The difficulty, of course, is in determining a value of γ^{n+1} that is consistent with the values of N^{n+1} and v^{n+1} . This could be an iterative process, or one could assume that the $\Delta\gamma$ will be small with respect to γ and proceed in the following manner. One already has the value of the deviatoric stress without any relaxation from

$$s_d^* = s_d^n + \frac{4}{3} \mu \frac{\dot{v}}{v} \Delta t^{n+1} \quad (13)$$

One may approximate the value of resolved shear stress as

$$\tau^{n+1} = \frac{3}{4} \text{ ABS} \left[s_d^* \right] \quad (14)$$

and the average dislocation velocity as

$$v^{n+1} = v_\infty \exp \left\{ - \frac{\tau_o + \phi \gamma^n}{\tau^{n+1}} \right\} \quad (15)$$

The dislocation density is obtained by

$$N^{n+1} = N_0 + \alpha (\gamma^n)^{\beta} \quad (16)$$

and the plastic shear-strain-rate by

$$\dot{\gamma}^{n+1} = b N^{n+1} v^{n+1} \quad (17)$$

From this one obtains the "relaxed" value of the deviatoric stress and the new value of plastic shear strain by the relations,

$$S_d^{n+1} = S_d^* + \frac{8}{3} \mu \dot{\gamma}^{n+1} \cdot \Delta t^{n+1}$$

and

$$\gamma^{n+1} = \gamma^n + \dot{\gamma}^{n+1} \Delta t^{n+1} \quad (18)$$

3. Comparison with Local* Shear Strain Calculation

One may wonder if this calculation and the one involving the local shear strain give the same results. To make this determination, two test problems with identical initial conditions and material properties were run. Both runs used the von Mises yield criterion in relaxation, making the two problems as identical as possible. The problem used a 1/8-inch driver plate of ARMCO iron with an initial velocity of 1.55×10^4 cm/sec. The target was 1/4-inch of ARMCO iron backed by a slab of quartz. A Lagrangian edit was taken just inside the quartz at the iron/quartz interface, and the observed waveform was used for the basis of comparison.

The material properties used for the iron were

$$\begin{aligned} \text{Bulk modulus} &= 9.05 \times 10^{11} \text{ dynes/cm}^2 \\ \text{Shear modulus} &= 8.12 \times 10^{11} \text{ dynes/cm}^2 \\ \text{Burgers vector} &= 2.5 \times 10^{-8} \text{ cm} \\ \text{Shear velocity} &= 3.22 \times 10^5 \text{ cm/sec} \\ \text{Initial dislocation density} &= 10^6 \text{ lines/cm}^2 \end{aligned}$$

*Local Shear Strain refers to that calculated at any instant in time, Eq. (5).

Coefficients:

$$\alpha = 1.0 \times 10^{11} \text{ lines/cm}^2$$

$$\beta = 1.0$$

$$\tau_0 = 1.98 \times 10^{10} \text{ dynes/cm}^2$$

Initial plastic shear strain = 0.

The quartz had an elastic modulus of 8.73×10^{11} dynes/cm². To allow the driver to separate from the target, an interface strength of 5 dynes/cm² was imposed.

In addition the incremental plastic shear strain model was employed to control the deviatoric stress in the unloading portion of the stress pulse. The results of the three calculations are shown in figure 4.

One notes some differences in the compressive portion of the wave for the local and incremental shear stress models. The local shear stress model has a higher relaxation rate, causing the upper-lower yield phenomenon to be less pronounced. Because the Burgers vector is constant, and v is calculated in the same fashion for both models, the only parameter that can be controlling the difference is the value of the plastic shear strain in the relationship for the dislocation density. Thus one must conclude that there is some difference in the two methods used. Because the difference is a cumulative effect in the incremental model, the magnitude for any given step could be relatively small and difficult to resolve. Also, the precision of the models used does not warrant extensive investigation of these differences.

A rather significant difference is noted between the unloading wave profile for the von Mises yield criterion and the rate dependent yield function. These differences have not been investigated at this writing, but a difference would be anticipated. A series of stress-versus-distance plots for different times are shown in the Appendix for the total plastic shear strain model with the von Mises yield criterion in unloading, and the differential plastic shear strain model for both loading and unloading. This gives the reader a better example of the total problem that produced the waveforms in figure 4.

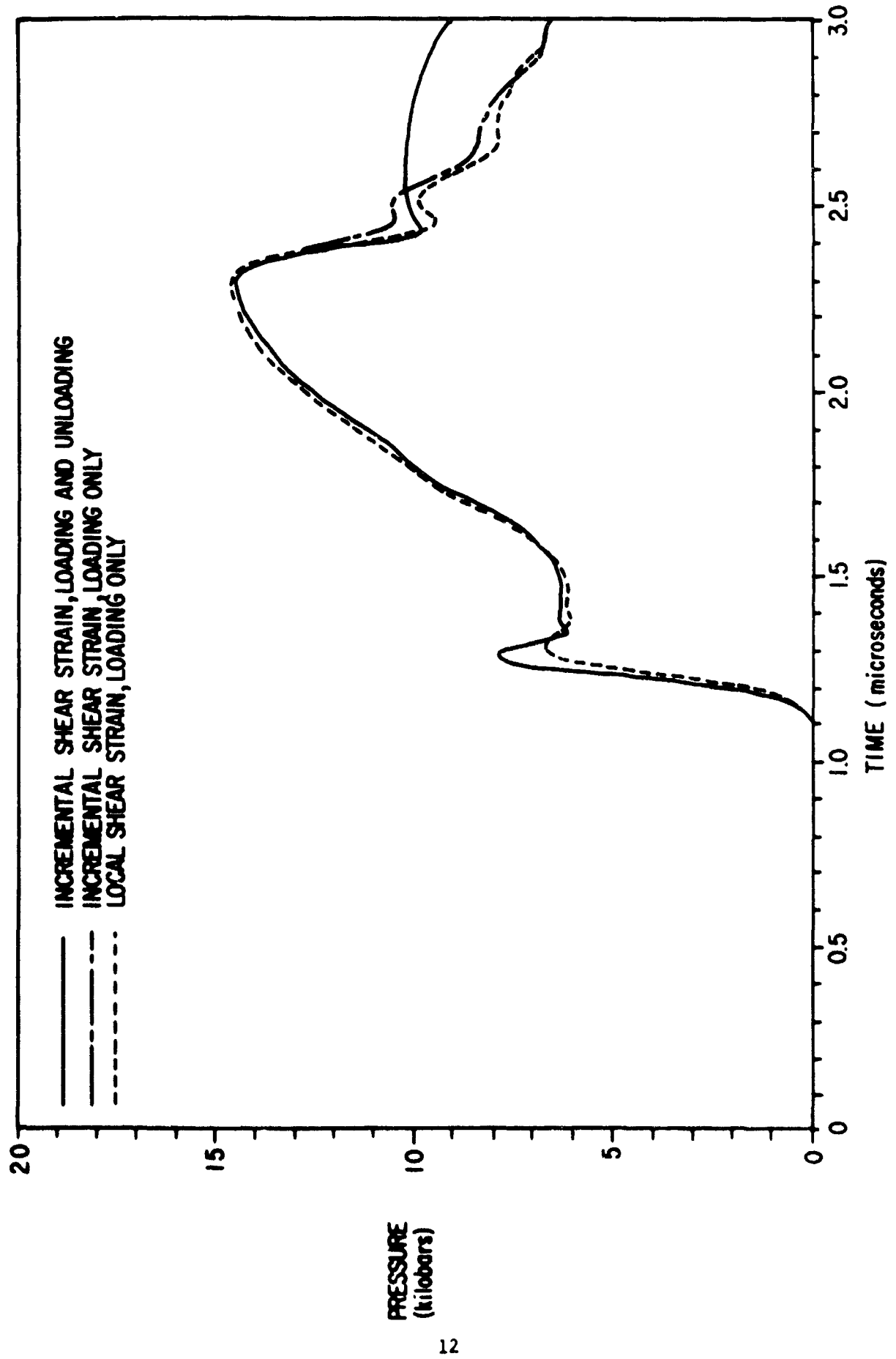


Figure 4. Comparison Between Waveforms Generated by Various Dislocation Models

SECTION III
STRESS-RELAXATION MODEL

Two models were developed in reference 3. One was a macroscopic model based upon a single characteristic relaxation time; the other, a microscopic model, used dislocation dynamics coupled with fairly complicated formulas for the rate of mobile and total dislocation production and disappearance. While the latter model is somewhat different from Taylor's, they both obtain γ from the mobile dislocation density and the average dislocation velocity. Thus, the other model chosen for programming into PUFF was the macroscopic relaxation model that employs a single parameter, the characteristic relaxation time, to produce a time-dependent stress deviator calculation.

This model uses the difference in the actual deviatoric stress computed and the equilibrium value calculated from the von Mises yield criterion along with the characteristic stress relaxation time. This formulation is simply stated as

$$\dot{s}_d = - \frac{\Delta\sigma}{T} \quad (19)$$

where $\Delta\sigma$ is the difference between the deviatoric stress and the equilibrium stress deviator based on a stress-dependent yield criterion, and T is the characteristic relaxation time. One must take into account whether or not the deviatoric stress is above the equilibrium yield value, and whether or not the material is loading or unloading. This is controlled by first checking the stress deviator in the normal manner to determine whether the yield condition is exceeded, and then, if the time-dependent relaxation is to be used, determining the new value of the deviator based upon Eq. (19). This equation is written for a given Lagrangian zone in PUFF as

$$\begin{aligned} s_d^{n+1/2} &= s_d^n + \frac{4}{3} \cdot \frac{\dot{v}}{v} \Delta t^{n+1} \\ s_d^{n+1} &= s_d^{n+1/2} - \left(s_d^{n+1/2} - n \cdot \frac{2}{3} \gamma \right) \cdot \frac{\dot{t}}{T} \end{aligned} \quad (20)$$

The variable θ is +1 on compression and -1 on unloading. This is determined within the stress-strain calculation, and is positive when the total stress is above the hydrostat. An interesting facet of this model is that it can be broken into a hydrostatic, elastic deviatoric, and plastic shear contribution to the total stress. One remembers from Eq. (1) that the time dependence of the total longitudinal stress was written as

$$\dot{\sigma} = \left(\lambda + \frac{2}{3} \mu \right) \dot{\epsilon} + \frac{4}{3} \mu \dot{\epsilon} - \frac{8}{3} \mu \dot{\gamma}$$

whereas in this model it becomes

$$\dot{\sigma} = \left(\lambda + \frac{2}{3} \mu \right) \dot{\epsilon} + \frac{4}{3} \mu \dot{\epsilon} - \frac{\left(s_d - \theta \frac{2}{3} y \right)}{T} \quad (21)$$

One may relate the last terms in Eq. (1) and (21) to find:

$$\frac{8}{3} \mu \dot{\gamma} = \frac{\left(s_d - \theta \frac{2}{3} y \right)}{T} \quad (22)$$

or that

$$\dot{\gamma} = \frac{3}{8\mu} \left[\frac{SD - \theta 2/3 y}{T} \right] \text{ for } |s_d| > \frac{2}{3} y \quad (23)$$

and

$$\dot{\gamma} = 0 \text{ for } |s_d| \leq \frac{2}{3} y$$

The plastic shear strain is given in Eq. (5) as

$$\gamma = \frac{3}{8\mu} \left[\left(\lambda + 2\mu \right) \epsilon - \dot{\gamma} \right]$$

so that the plastic shear strain rate is

$$\dot{\gamma} = \frac{3}{8\mu} \left[\left(\lambda + 2\mu \right) \epsilon - \dot{\sigma} \right] \quad (24)$$

One can see that there is dimensional equivalence between equations 23 and 24; however, the time dependence of the quantities is based upon different physical properties. One can also envision a value of T which causes the relaxation rate to become too large for the stability criterion in PUFF. This will occur when T is smaller than the time step in the problem. Thus one must use caution in choosing T , to insure that it is always greater than the anticipated time step.

1. Test Problems

The same impact conditions were used here with the comparison runs as were performed on the dislocation model. The relaxation time was varied between 10^{-4} and 10^{-8} seconds, and the variation in the waveshapes measured at Lagrangian edit are shown in figure 5. Since one must keep the relaxation time larger than the time step for stability, no lower values were used. One observes that these effects are somewhat different than the effects seen from the dislocation model.

2. Programming Changes in PUFF

Relatively few changes are required in the PUFF code to input the two models discussed. The material variables must be read in with the GENRAT routine, and placed in the common block. The only changes required in the program are in the HYDRO subroutine, and occur in the stress-strain calculation. The parameters used are

BURG(M) = Burgers vector, (lines/cm²)
CSHR(M) = Acoustic shear velocity, (cm/sec)
TAU0(M) = τ_0 in equation 4, (dynes/cm²)
ALFR(M) = α in equation 3, (lines/cm²)
BETA(M) = β in equation 3, (dimensionless)
ANO(M) = Initial dislocation density, (lines/cm²)
FEE(M) = ϕ in equation 4, (dynes/cm²)
TRELAX(M) = Characteristic relaxation time for macroscopic model, (sec)

The changes to the stress-strain calculation are shown in figure 6; the general flow of the calculation is shown in figure 1. The new variable names were chosen for ease of understanding with respect to the equations previously discussed.

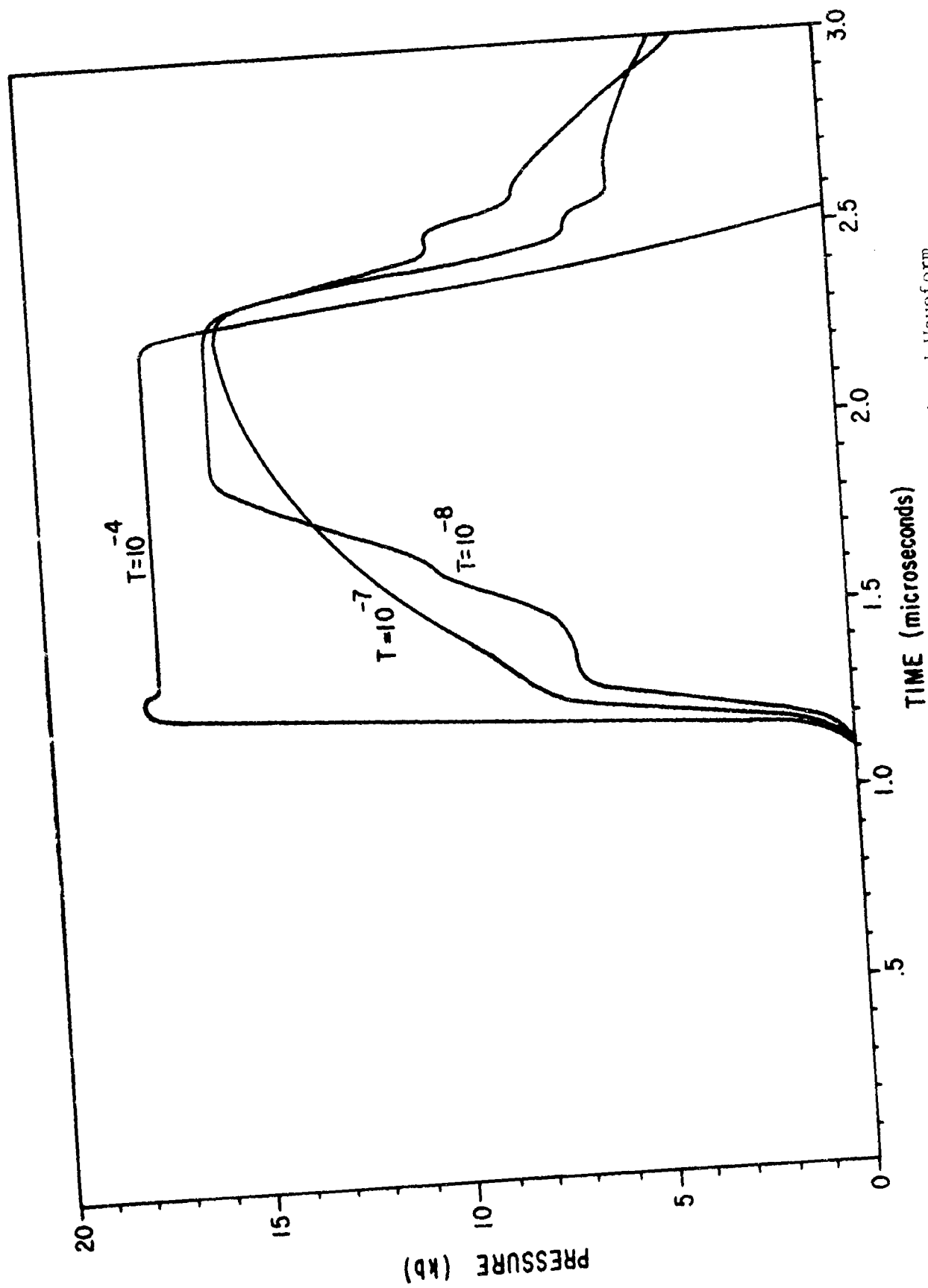


Figure 5. Effect of Relaxation Time Upon a Transmitted Waveform

```

C      STRESS-STRAIN CALCULATION
C      VELS=DV*DAVG
C      THETA=-SD(J)/AMAX1(1.0, ABS( SD(J) ))
C      STRAIN=1.0-RHO(M)/D(J)
C      FMU=D(J)/DHO(M)-1.
C      BULK=EQSTC(M)
C      IF(STRAIN.GT.C.) RULK=((EQSTS(M)*FMU+EQSTR(M))*FMU+EQSTS(M))*FMU/S
C
1TPAIN
      VAMU=4.0/3.*AMU(M)*BULK/EQSTC(M)
      IF(VAMU-4.0/3.*AMU(M)) 150.151.151
      VAMU=A.0/3.*AMU(M)
      SD(J)=SD(J)+VAMU*VELS
      CSHP=SOPT(.75*VAMU/D(J),
      IF(FURG(M).LE.0.) GO TO 110
      EF1=.75*ABS(SD(J))
      IF(FF1.LE.10.) GO TO 110
      ANI=ANO(M)+ALFR(M)*GAMFR(J)**BETA(M)
      VDIS=CSHR*EXP(-(TAUO(M)+FEE(M))*GAMER(J)/EF1)
      GAMADT=FURG(M)*ANI*VDIS
      GO TO 111
      VMC=3.0/2.*SD(J)*SD(J)
      EMU=D(J)/DHO(M)-1.
      IF(VMC-2.0/3.*Y0Z(J)*Y0Z(J)) 110.110.9
      Y0Z(J)=Y0Z(J)+YADD(M)*ANS(DV)*(J)*DOLD/RHO(M)/(2.*YMU(M))
      IF(VMC-2.0/3.*Y0Z(J)*Y0Z(J)) 111.111.11
      IF(TRFLAX(M).LE.0.) GO TO 112
      WY=.2.*Y0Z(J)
      IF(THFTA.LE.0.) WY=0.
      GAMADT=ARS(.5/VAMU*(SD(J)+THFTA*WY)/TRFLAX(M))
      SD(J)=SD(J)+2.*VAMU*GAMADT*DTNH*THFTA
      GAMFR(J)=GAMER(J)+GAMADT*DTNH
      GO TO 10
      SD(J)=SD(J)*Y0Z(J)*SQRT(?./(3.*VMC))
10    CONTINUE

```

Figure 6. Stress-Strain Routine Modified to Include Macroscopic Relaxation and Dislocation Dynamics Models for Strain-Rate Dependence

SECTION IV

DISCUSSION

The models incorporated into the code may serve as a skeletal framework that may be varied to approximate different phenomena relating to the strain rate dependent behavior of materials under impulsive loads. The macroscopic model may be employed either as used for the runs shown in this report with the yield strength below the hydrostat set to zero, or for any other variation desired. One may also choose to make the yield strength time dependent as discussed in reference 3. These changes are easily made in the stress-strain calculation presented in figure 6.

The dislocation dynamics model is based upon Eq. (2), and the expressions used for determining the dislocation density (mobile or total) and the dislocation velocity (mobile or average) may be modified by changing the expressions for the variables ANI and VDIS, respectively. The initial value of the plastic shear strain and the dislocation density should certainly be properly matched if they are to be used meaningfully. One can get some idea of the effect upon the calculation if the initial plastic shear strain is non-zero by examining figure 7. Here a comparison is made between the Lagrangian edit in the quartz for runs using initial plastic shear strain values of zero and 1 percent. By allowing the material to have been previously "cold worked" to the 1 percent value, a common practice with mild steels, one finds that the upper-lower yield phenomenon no longer appears in the propagated stress wave. The effects of the various other parameters upon a waveshape have been lightly touched on previously; however, the user should familiarize himself with their significance by performing a comprehensive sensitivity study on the parameters of whichever model he chooses to employ.

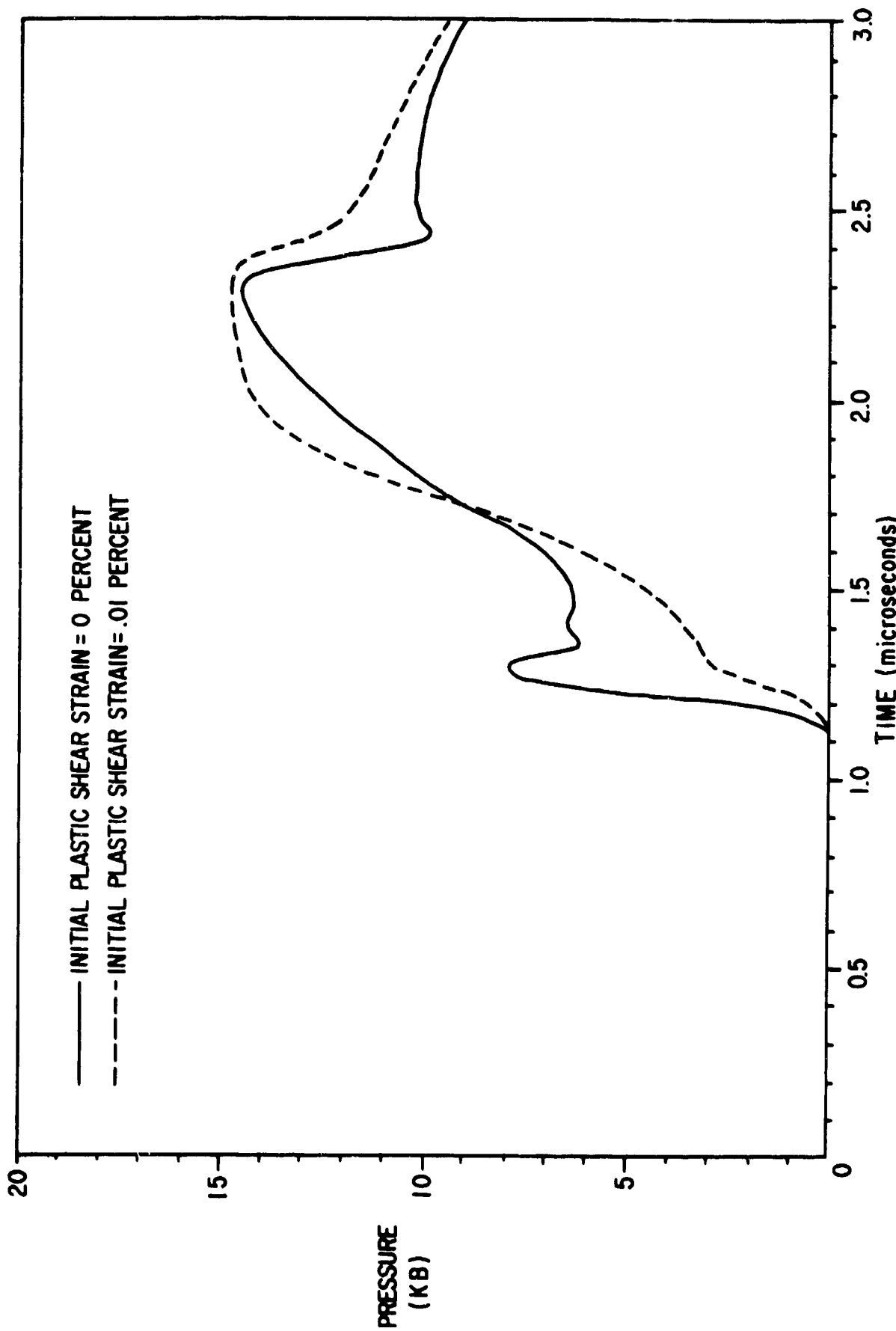


Figure 7. Illustration of the Effect of the Initial Value of Plastic Shear Strain on a Propagated Waveform

SECTION V
CONCLUSIONS

Based upon the computed stress waves presented for the two strain-rate dependent material response models employed, the following conclusions are drawn:

1. More realistic descriptions of the response of crystalline materials are possible by employing deviatoric stress calculations, to account for microscopic behavior in the PUFF code.
2. The flexibility of the models presented provides a more physically realistic description of material response of impulsive loads and necessitates more precise definition of the material's microscopic behavior for these descriptions to have any real meaning.
3. The microscopic model employs enough parameters to make concise definition of the effect of any single parameter upon a propagated stress wave virtually impossible.

APPENDIX

Two of the computer runs described in the report are more fully presented here. A series of stress-versus-distance waveforms are displayed for both the incremental plastic shear strain model used for loading and unloading, and for the local plastic shear strain model. The cycle numbers and problem times associated with each plot appear at the top of each margin. Figures 8 through 12 are the results for the incremental plastic shear strain problem, and figures 13 through 17 are from the local plastic shear strain problems.

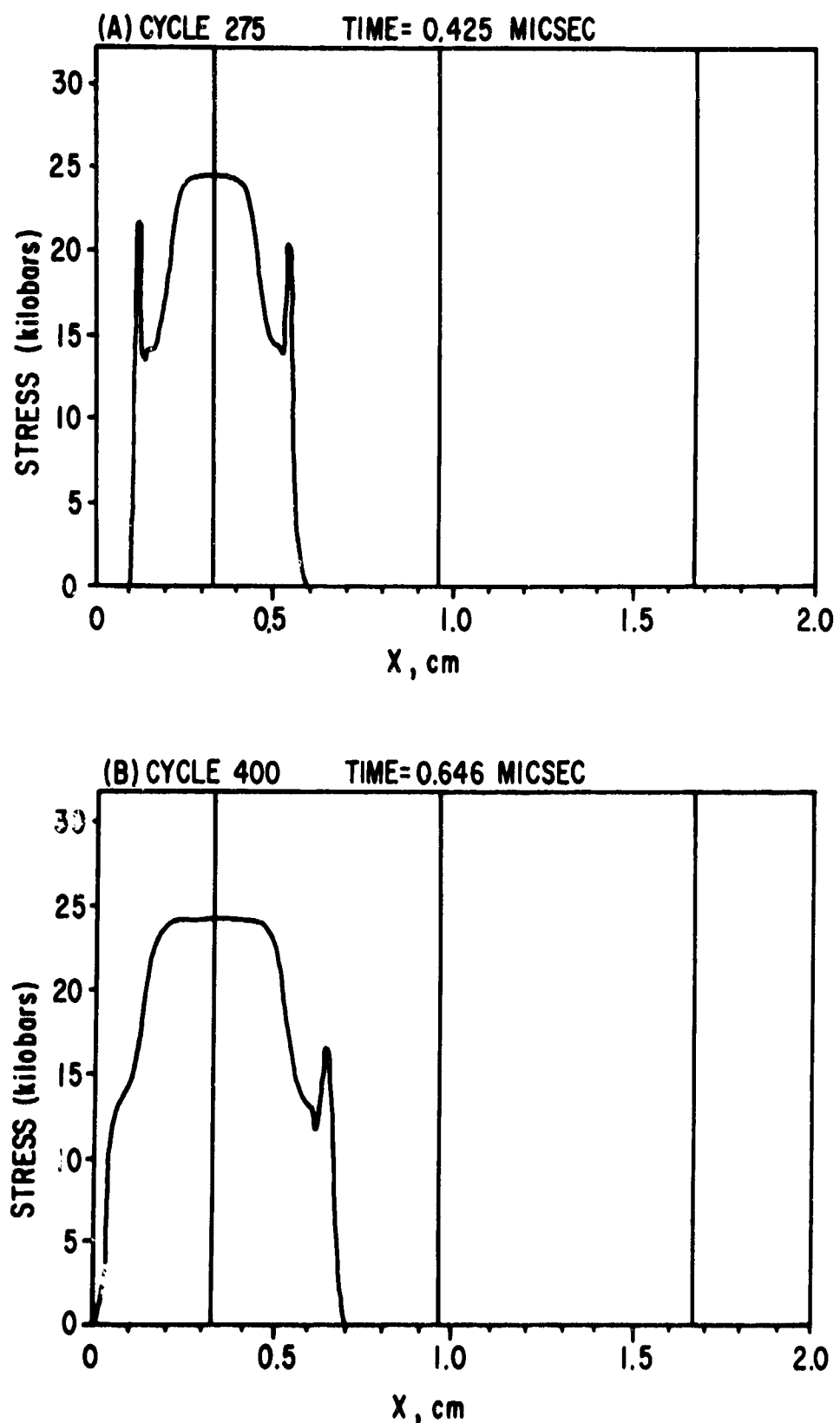


Figure 8. Stress-Distance Histories for Incremental Shear Strain Problem

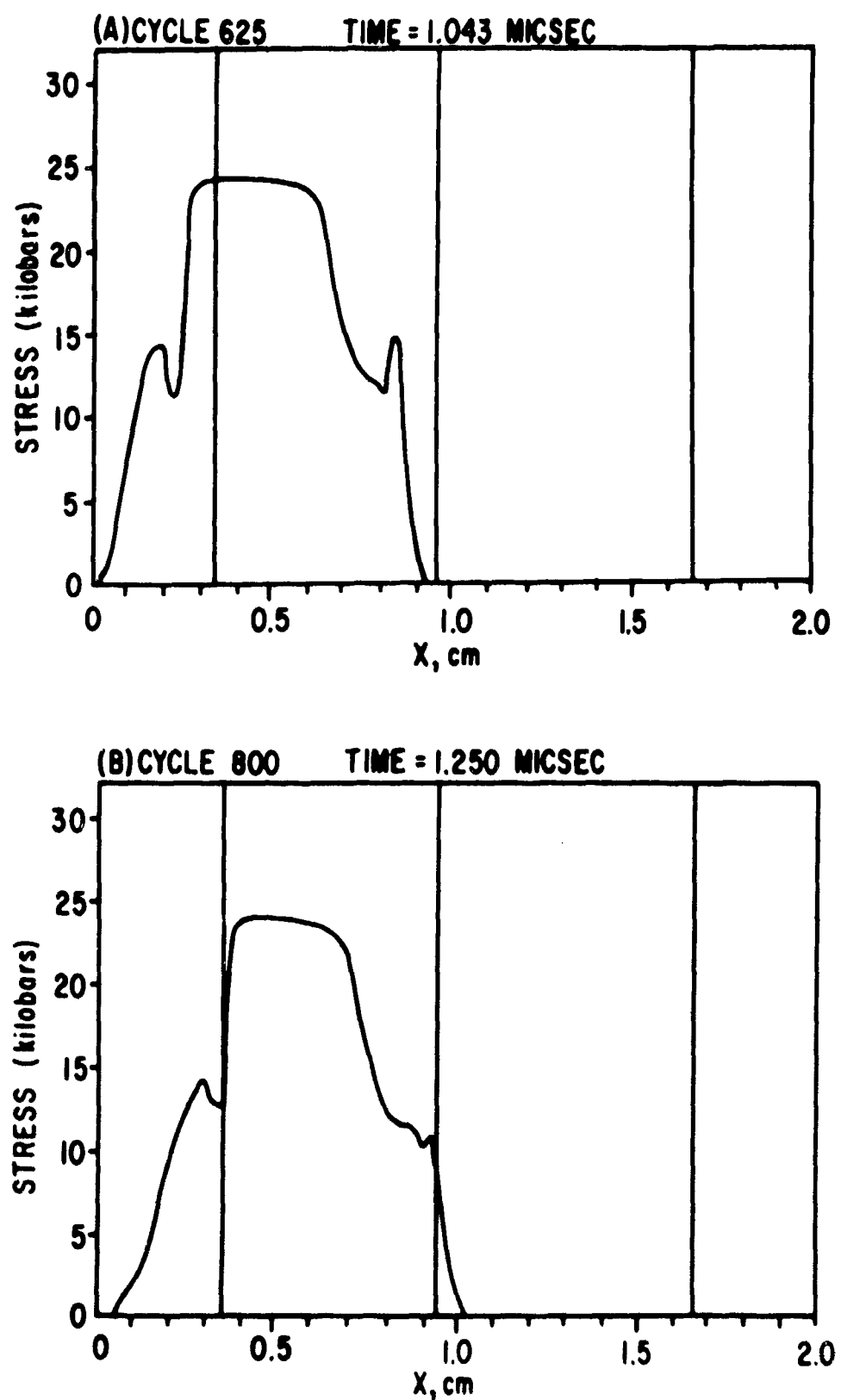


Figure 9. Stress-Distance Histories for Incremental Shear Strain Problem

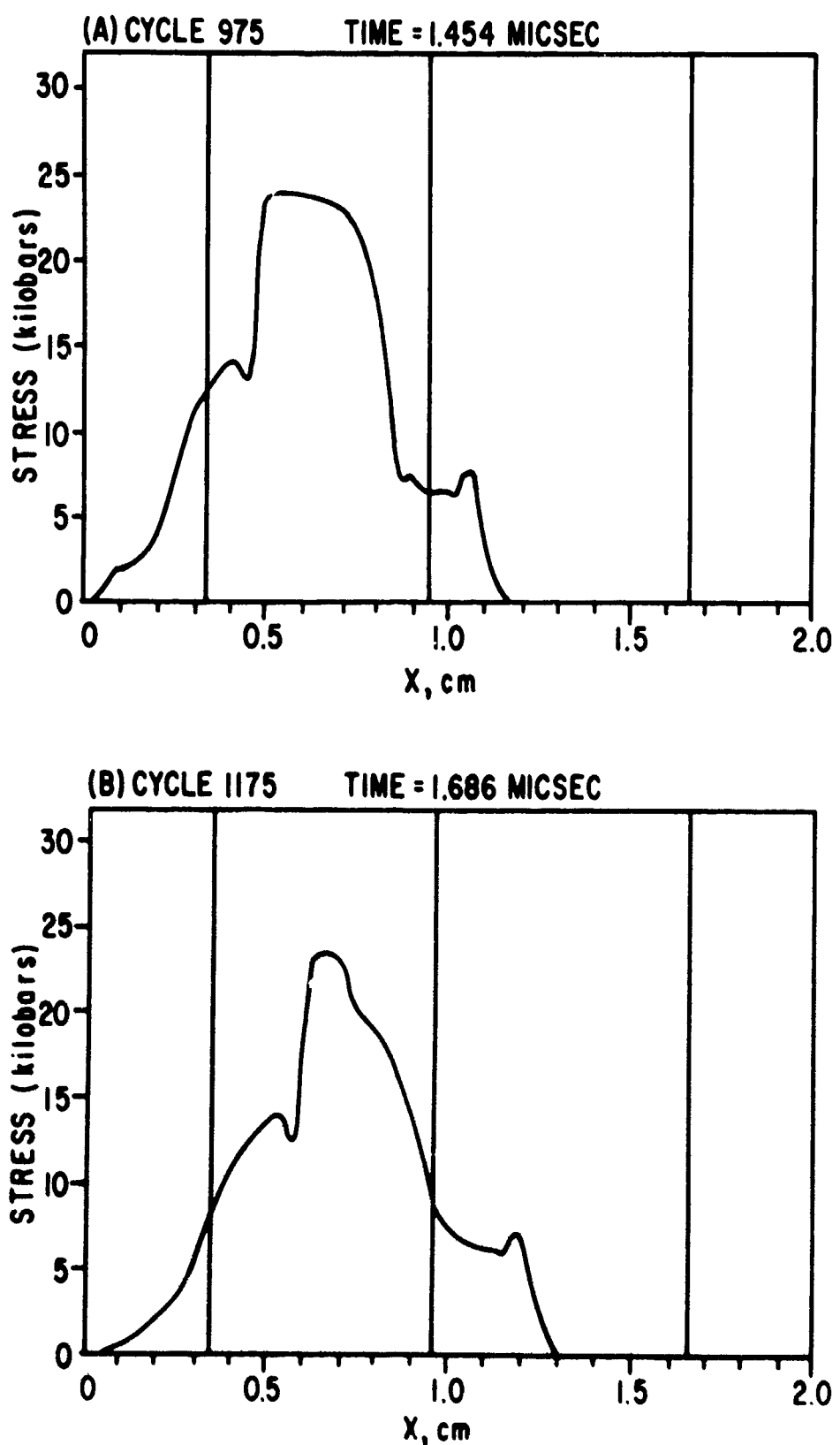


Figure 10. Stress-Distance Histories for Incremental Shear Strain Problem

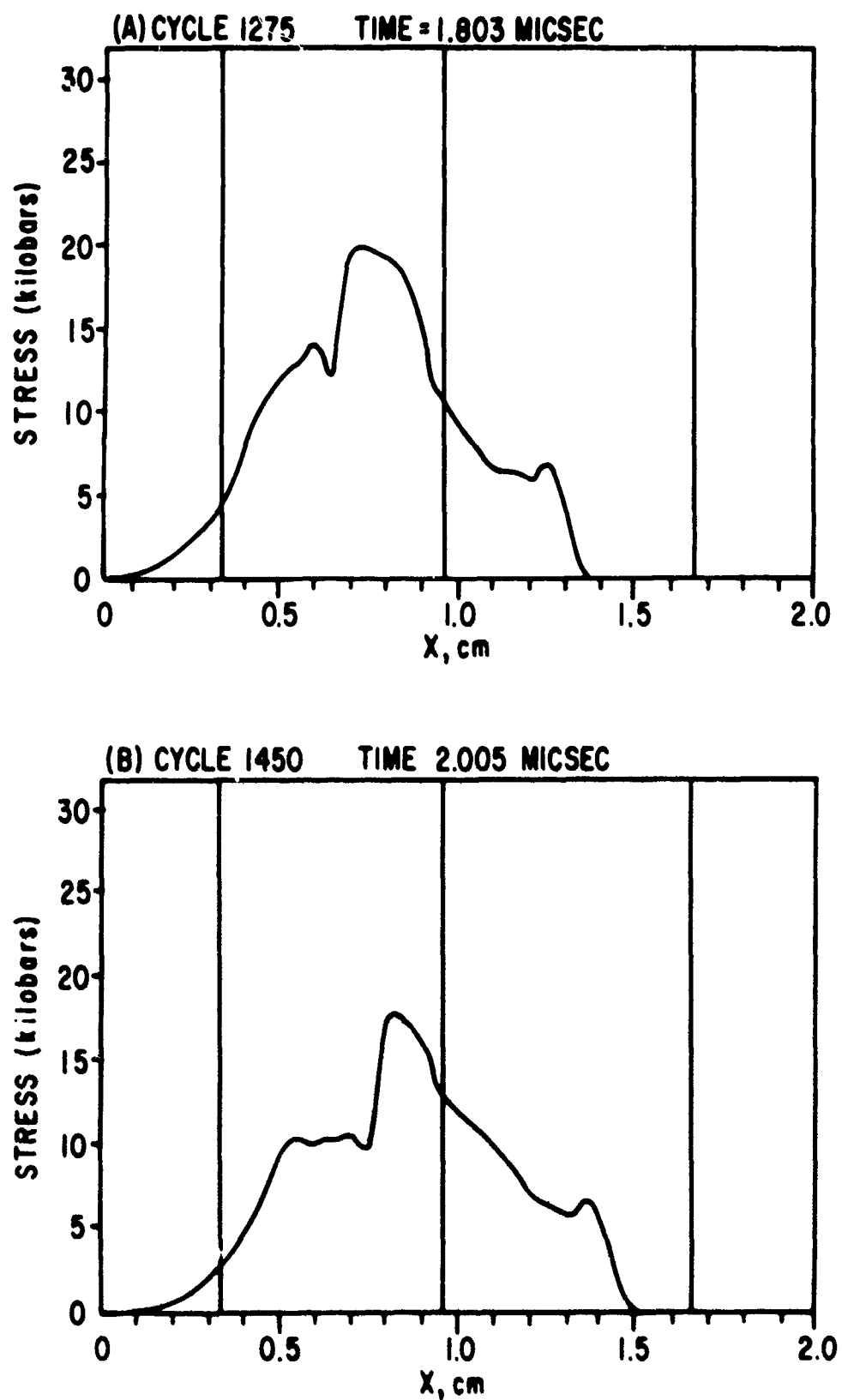


Figure 11. Stress-Distance Histories for Incremental Shear Strain Problem

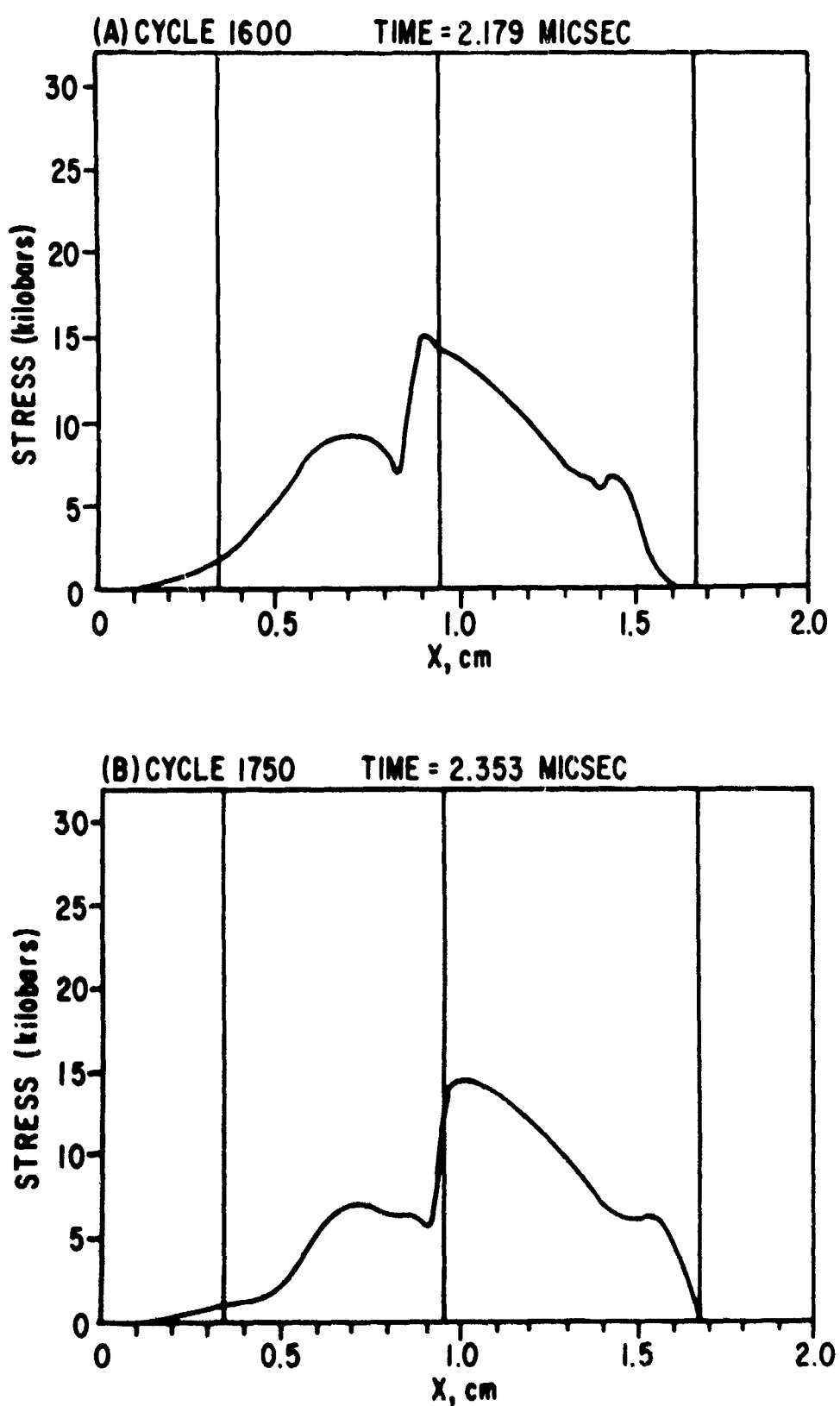


Figure 12. Stress-Distance Histories for Incremental Shear Strain Problem

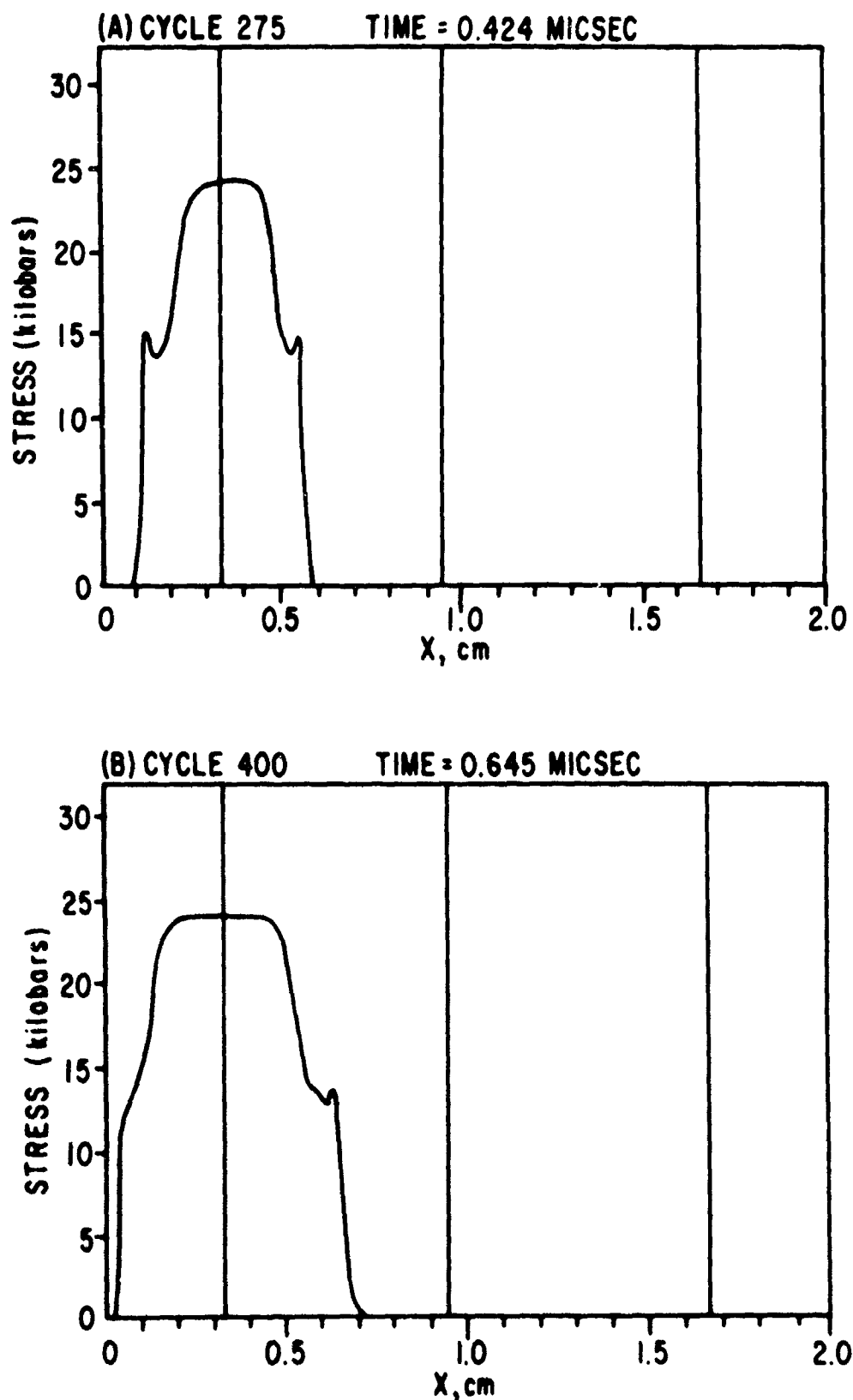


Figure 13. Stress-Distance Histories for Local Shear Strain Problem

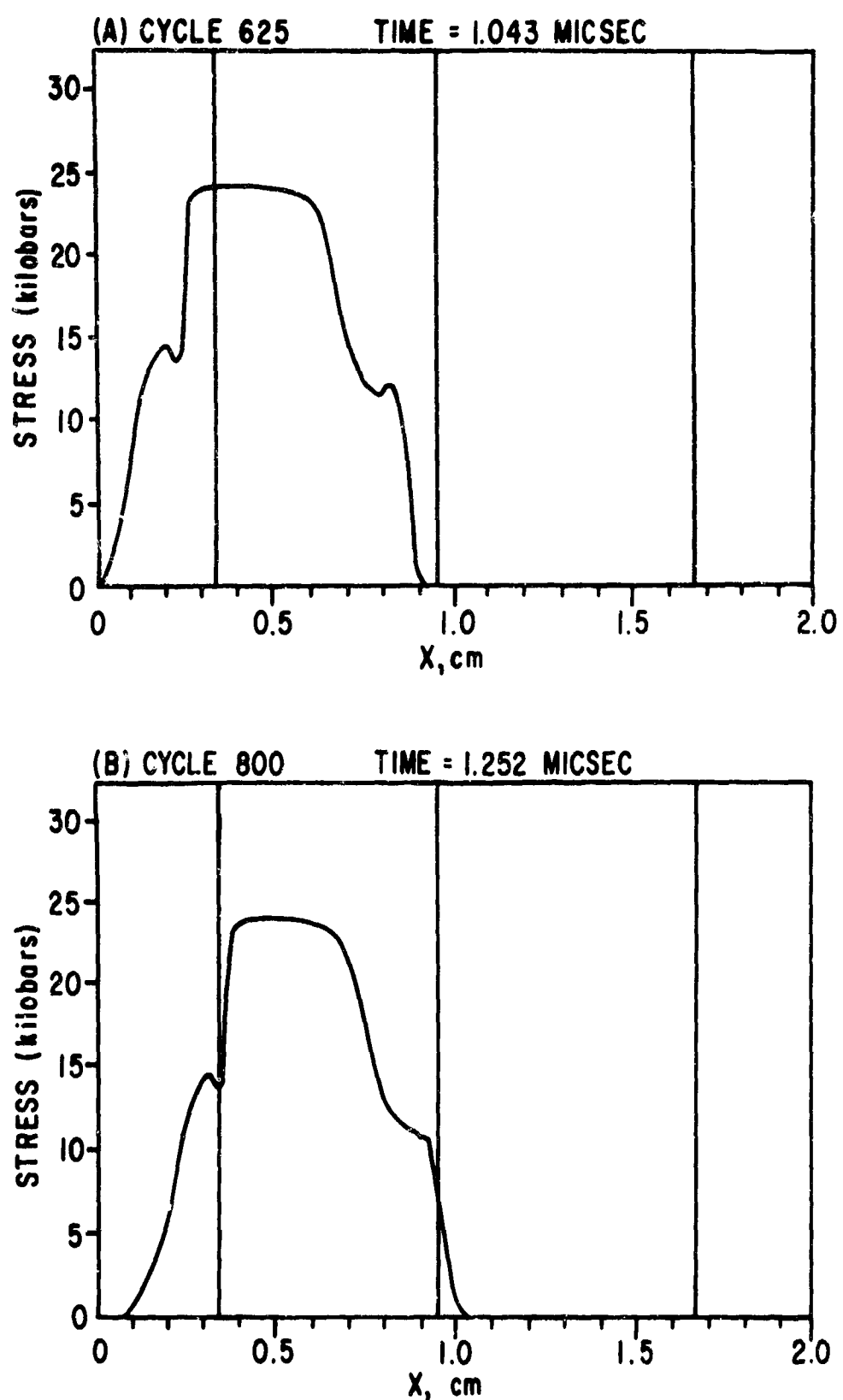


Figure 14. Stress-Distance Histories for Local Shear Strain Problem

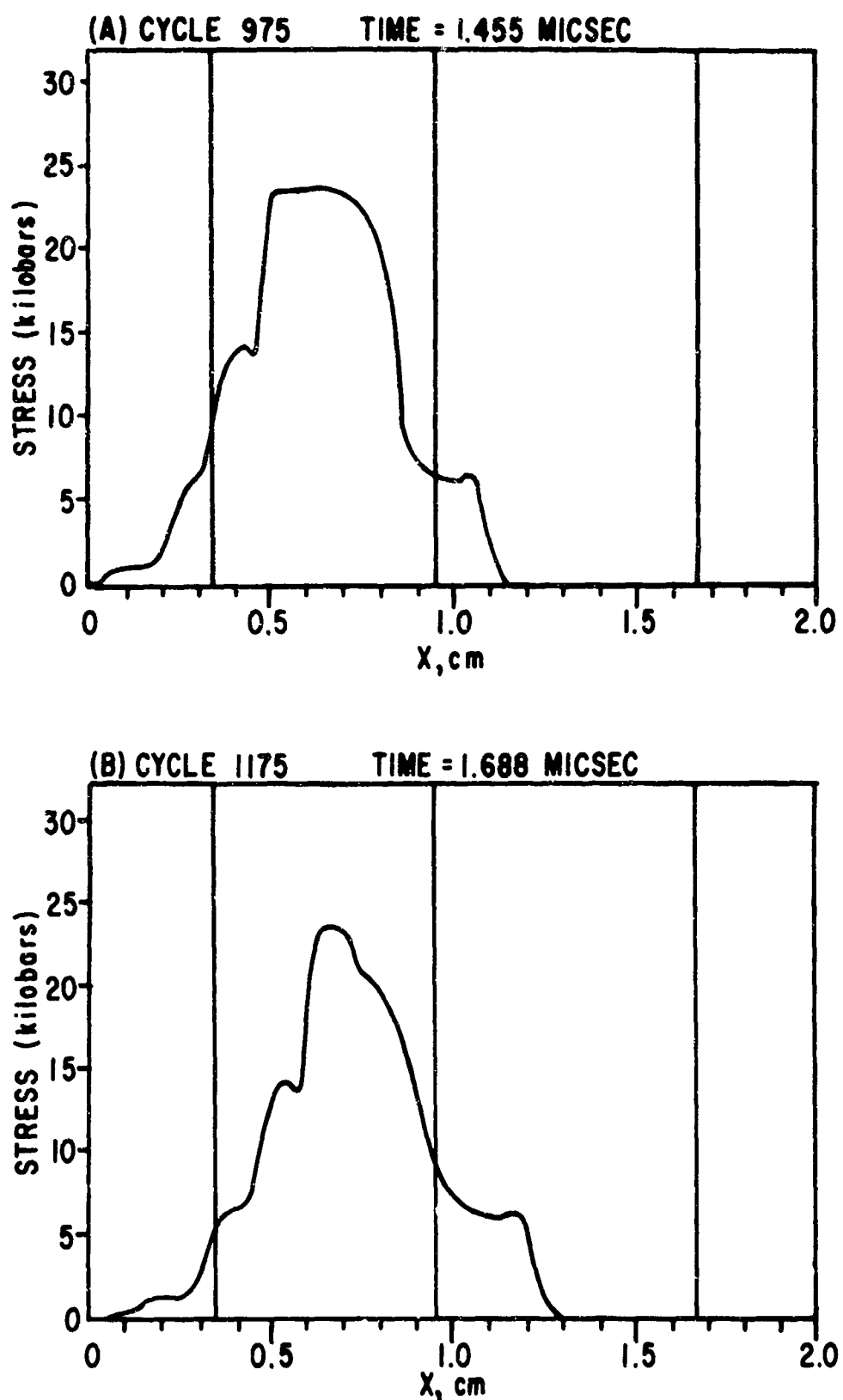


Figure 15. Stress-Distance Histories for Local Shear Strain Problem

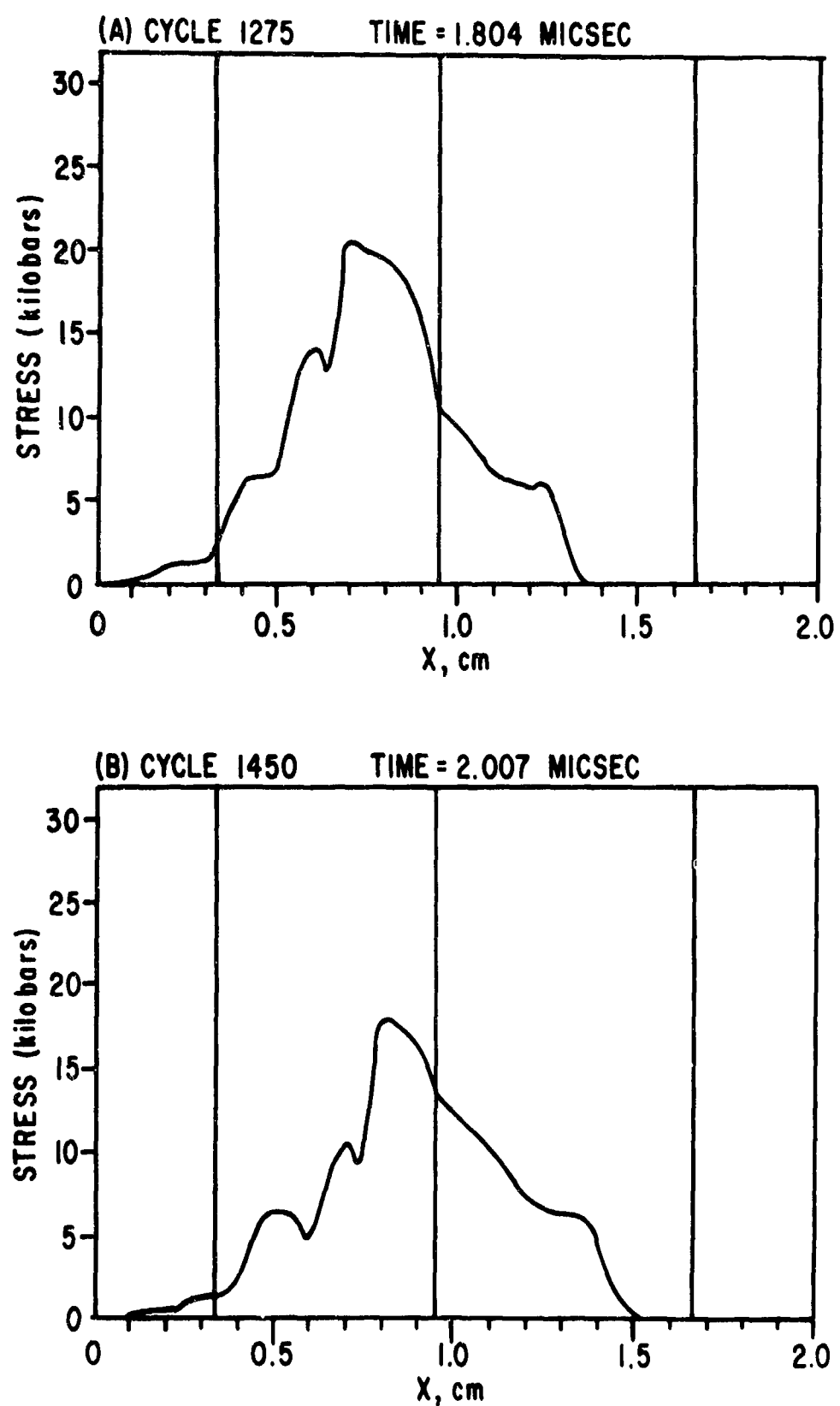


Figure 16. Stress-Distance Histories for Local Shear Strain Problem

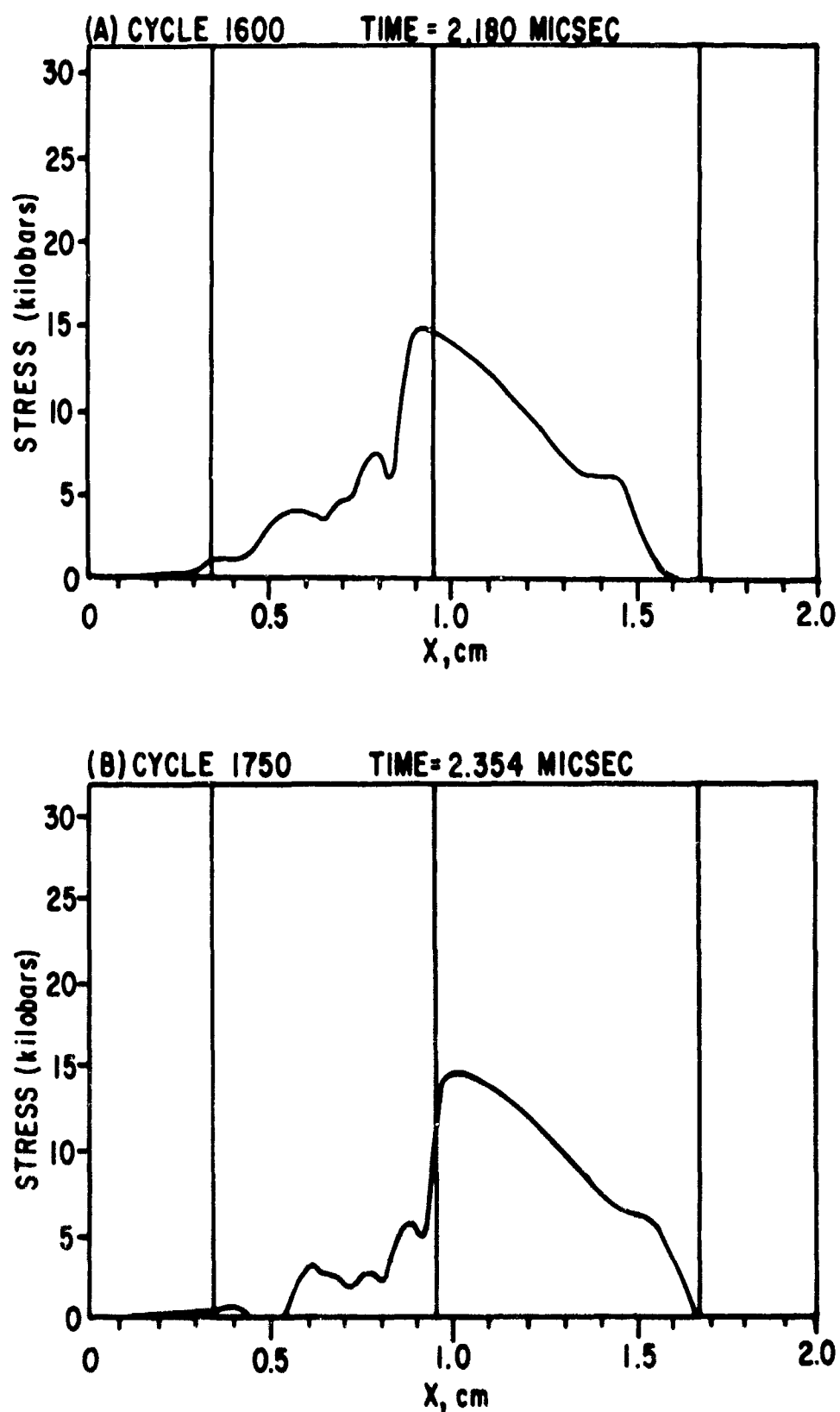


Figure 17. Stress-Distance Histories for Local Shear Strain Problem

REFERENCES

1. Brodie, R. N., Hormuth, J. E., The PUFF 66 and P PUFF 66 Computer Programs, AFWL-TR-66-48 (AD 483 409), Air Force Weapons Laboratory, Kirtland AFB, NM, May 1966.
2. Wilkins, M. L., Calculation of Elastic-Plastic Flow, Lawrence Radiation Laboratory, California, UCRL 7322, 1963.
3. Taylor, J. W., "Dislocation Dynamics and Dynamic Yielding," Journal of Applied Physics, 36, pp. 3146-3150, 1965.
4. Anderson, G. D., Murri, W. D., Alverson, R. C., Hanagud, S. V., Stress Relaxation in the Shock Compression of Solids, AFWL-TR-67-24 (AD 814 787), Air Force Weapons Laboratory, Kirtland AFB, NM, May 1967.
5. Gilman, J. J., Johnston, W. G., "Dislocation Velocities, Dislocation Densities, and Plastic Flow in Lithium Fluoride Crystals," Journal of Applied Physics, 30, pp. 129-144, 1959.
6. Keh, A. S., Weissmann, S., Proceedings on the Conference on Electron Microscopy and Strength of Materials, edited by G. Thomas and J. Washburn, Interscience Publishers, Inc., 1963.

UNCLASSIFIED

Security Classification

DOCUMENT CONTROL DATA - R & D

(Security classification of title, body of abstract and indexing annotation must be entered when the overall report is classified)

1. ORIGINATING ACTIVITY (Corporate author) Air Force Weapons Laboratory (WLRP) Kirtland Air Force Base, New Mexico 87117	2a. REPORT SECURITY CLASSIFICATION UNCLASSIFIED
	2b. GROUP

3. REPORT TITLE

THE INCLUSION OF STRAIN-RATE DEPENDENCE IN THE PUFF COMPUTER CODE

4. DESCRIPTIVE NOTES (Type of report and inclusive dates)

September 1968 through January 1969

5. AUTHOR(S) (First name, middle initial, last name)

Capt Joseph B. Webster, III

6. REPORT DATE

March 1969

7a. TOTAL NO. OF PAGES

42

7b. NO. OF REPS

6

8a. CONTRACT OR GRANT NO.

8b. ORIGINATOR'S REPORT NUMBER(S)

8. PROJECT NO. 5710

AFWL-TR-69-11

cSubtask: AA 106

9b. OTHER REPORT NO(S) (Any other numbers that may be assigned this report)

d.

10. DISTRIBUTION STATEMENT This document is subject to special export controls and each transmittal to foreign governments or foreign nationals may be made only with prior approval of AFWL (WLRP), Kirtland AFB, NM 87117. Distribution is limited because of the technology discussed in the report.

11. SUPPLEMENTARY NOTES

12. SPONSORING MILITARY ACTIVITY

AFWL (WLRP)

Kirtland AFB, NM 87117

13. ABSTRACT

(Distribution Limitation Statement No. 2)

Two mathematical descriptions of the strain-rate dependence of materials response to suddenly applied one-dimensional strain loads were incorporated into the PUFF wave propagation computer codes. The models are quite different in that one uses a macroscopic relaxation time to govern the stress-relaxation rates, while the other uses the microscopic theories of dislocation dynamics. The results of several sample calculations are discussed, and the changes required in the programming sequence are given. Some comments are provided concerning the validity and usefulness of these models, and a brief analysis of the effects of parametric variations is presented.

DD FORM 1 NOV 68 1473

REPLACES DD FORM 1473, 1 JAN 64, WHICH IS
OBSOLETE FOR ARMY USE.

UNCLASSIFIED

Security Classification

UNCLASSIFIED

Security Classification

14. KEY WORDS	LINK A		LINK B		LINK C	
	ROLE	WT	ROLE	WT	ROLE	WT
Finite difference calculations Wave propagation Strain-rate effects Shock waves Elastic-plastic						

UNCLASSIFIED

Security Classification